A FINITE THICKNESS INTERFACE ELEMENT FOR COMPOSITE DELAMINATION

J. Reinoso[1], M. Paggi[2], A. Blázquez[1]

[1]Elasticity and Strength of Materials Group, School of Engineering, Universidad de Sevilla, Camino de los Descubrimientos s/n, 41092, Seville, Spain
Email: jreinoso@us.es, abg@us.es, Web Page: http://www.germus.es
[2]IMT Institute for Advanced Studies Lucca, Piazza San Francesco 19, 55100 Lucca, Italy
Email: marco.paggi@imtlucca.it, Web Page: http://musam.imtlucca.it/

Keywords: Interface Model, Delamination, Composite structures,

Abstract
Delamination and decohesion failure notably affect the integrity of composite structures and therefore there exist a concurrent need for developing reliable numerical tools that can accurately simulate such events under mixed-mode loading conditions. This work presents a novel finite thickness interface element for delamination analysis of composites structures based on the solid shell concept undergoing finite strains. With respect to the inelastic behavior of the interface, an extension of the so-called Linear Elastic Brittle Interface Model (LEBIM) is proposed. A preliminary benchmark simulation assesses the practicability of the proposed formulation.

1. Introduction

Damage tolerance is a current demand with regard to in service behavior of modern composite structures. In this context, the development of advanced numerical models simulating decohesion and/or delamination in such specimens has been a matter of increasing interest in the research community over the last few years.

These inelastic processes have been widely modeled using different numerical strategies, such as the so-called virtual crack closure technique (VCCT) [1], the Cohesive Zone Models (CZMs) [2, 3], and more recently the so-called Linear Elastic Brittle Interface Model (LEBIM) [15]. The latter is one of the most popular approaches to trigger and simulate such fracture events. Their popularity over other techniques is mainly motivated by their high versatility and relative simplicity in terms of numerical implementation. Cohesive zone model formulations are characterized an inelastic traction-separation law (TSL) which governs the interface degradation along the loading application.

Finite elements based on cohesive zone models are usually implemented in zero-thickness or surface-like interface elements, see, e.g., the bi-linear CZM [4, 5], the exponential CZM [6, 7], following continuum-based formulations [8], among many others. Recently, several authors have proposed the incorporation of geometrically nonlinear effects in the description of the interface failure, see [9, 10] and the references therein given.

One conceivable alternative to the previously mentioned zero-thickness methods regards the idealization of the interface between two bodies with an initial finite thickness [11–13]. This approximation

Excerpt from ISBN 978-3-00-053387-7

allows the description of the interface using a pseudo-continuum approach. The current investigation is concerned with the development of a novel cohesive finite thickness interface element for delamination analysis of composites structures. Differing from previous investigations, the current formulation relies on a degenerated version of the so-called solid-shell concept [14], attaining both geometrical and material nonlinearities. The current formulation is especially suitable for thin-walled applications, which are of major interest in composites. With regard to the TSL, an extension of the so-called LEBIM [15] is integrated into the current interface element. A benchmark application is shown to assess the practicability of the developed interface model.

2. Finite thickness interface model

Let us to consider two adjacent bulks $\mathscr{B}_0^{(i)}$ with $i = 1, 2$ in the reference configuration, which correspond to the bulks $\mathscr{B}_t^{(i)}$ in the current configuration, respectively, see Figure 1. Between these two bodies, an interface of finite thickness is assumed to exist. This interface constitutes the region of interest in the sequel (see Figure 1), whose reference configuration is denoted by $\bar{\mathscr{B}}_0$. The nonlinear deformation map is identified by $\boldsymbol{\varphi}(\mathbf{X}) : \bar{\mathscr{B}}_0 \times [0, t] \rightarrow \mathbb{R}^3$, where $[0, t]$ is the time step interval, that maps the reference material points ($\mathbf{X} \in \bar{\mathscr{B}}_0$) onto the current material points ($\mathbf{x} \in \bar{\mathscr{B}}$) [1].

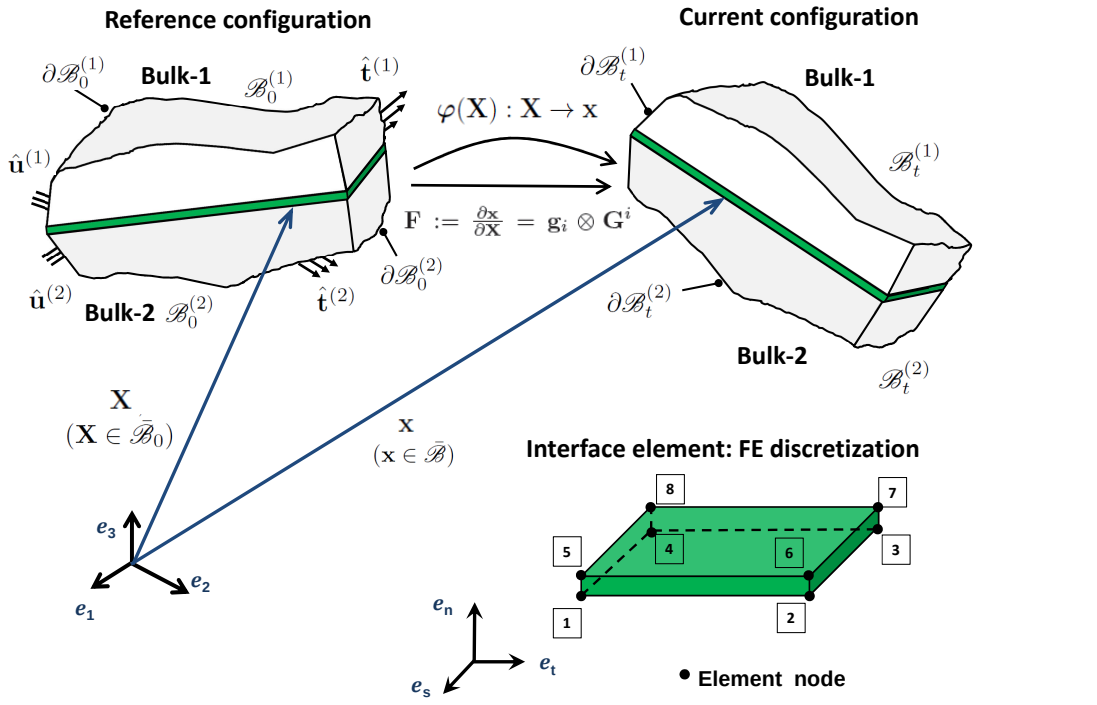

Figure 1. Geometric definition of the interface between the two bulk bodies in the reference and current configurations. Discretization of the three-dimensional finite thickness interface element.

The interface, where fracture events are confined to occur, is idealized under the assumption that the thickness dimension is significantly smaller than the in-plane dimensions [11]. The local curvilinear covariant convected basis in the reference and in the current configurations of the interface are respectively defined as:

$$\mathbf{G}_a = \frac{\partial \mathbf{X}(\boldsymbol{\xi})}{\partial \xi^a}; \quad \mathbf{g}_a = \frac{\partial \mathbf{x}(\boldsymbol{\xi})}{\partial \xi^a}, \quad a = s, t, n \tag{1}$$

[1] In the following, magnitudes in capital and small letter are referred to the reference and current configurations, respectively.

Excerpt from ISBN 978-3-00-053387-7

where the subscripts s and t identify the in-plane directions and the subscript n stands for the magnitudes referred to the out of plane direction.

The vectors perpendicular to the interface midsurface in the reference and the current configurations are defined as:

$$\bar{\mathbf{G}}_n = \frac{\bar{\mathbf{G}}^n}{\bar{G}^{nn}}, \quad \text{where } \bar{\mathbf{G}}^n = \mathbf{G}_s \times \mathbf{G}_t;\ \bar{G}^{nn} = \bar{\mathbf{G}}^n \cdot \bar{\mathbf{G}}^n. \tag{2}$$

$$\bar{\mathbf{g}}_n = \frac{\bar{\mathbf{g}}^n}{\bar{g}^{nn}}, \quad \text{where } \bar{\mathbf{g}}^n = \mathbf{g}_s \times \mathbf{g}_t;\ \bar{g}^{nn} = \bar{\mathbf{g}}^n \cdot \bar{\mathbf{g}}^n. \tag{3}$$

The update of the current configuration is obtained through the use of the displacement field $\mathbf{u}$ as follows: $\mathbf{x}(\boldsymbol{\xi}) := \mathbf{X}(\boldsymbol{\xi}) + \mathbf{u}(\boldsymbol{\xi})$ (see Figure 1). The Jacobi matrices corresponding to the transformations between parametric space at the reference ($\mathbf{J}(\boldsymbol{\xi})$) and current ($\mathbf{j}(\boldsymbol{\xi})$) configurations render:

$$\mathbf{J}(\boldsymbol{\xi}) = [\mathbf{G}_s, \mathbf{G}_t, \mathbf{G}_n]^{\mathrm{T}}, \quad \mathbf{j}(\boldsymbol{\xi}) = [\mathbf{g}_s, \mathbf{g}_t, \mathbf{g}_n]^{\mathrm{T}}. \tag{4}$$

The deformation gradient takes the form:

$$\mathbf{F} := \nabla_{\mathbf{X}} \boldsymbol{\varphi} = \frac{\partial \mathbf{x}}{\partial \mathbf{X}} = \frac{\partial \mathbf{x}}{\partial \xi^a} \frac{\partial \xi^a}{\partial \mathbf{X}} = \mathbf{g}_a \otimes \mathbf{G}^a \tag{5}$$

where $\nabla_{\mathbf{X}}$ denotes the material gradient operator. The Green-Lagrange strain tensor is defined as:

$$\bar{\mathbf{E}} := \frac{1}{2}\left[\mathbf{F}^{\mathrm{T}}\mathbf{F} - \mathbb{I}_2\right] \tag{6}$$

where $\mathbb{I}_2$ stands for the second order identity tensor.

The reduced version of the Green-Lagrange strain tensor associated with the interlaminar strain components and their corresponding energetically conjugated stress components (corresponding to the second Piola-Kirchhoff stress tensor $\bar{\mathbf{S}}$) read:

$$\bar{\mathbf{E}} = \begin{bmatrix} \gamma_{sn} \\ \gamma_{tn} \\ e_{nn} \end{bmatrix} = \begin{bmatrix} \mathbf{g}_s \cdot \mathbf{g}_n - \mathbf{G}_s \cdot \mathbf{G}_n \\ \mathbf{g}_t \cdot \mathbf{g}_n - \mathbf{G}_t \cdot \mathbf{G}_n \\ \mathbf{g}_n \cdot \mathbf{g}_n - \mathbf{G}_n \cdot \mathbf{G}_n \end{bmatrix} = \begin{bmatrix} g_{sn} - G_{sn} \\ g_{tn} - G_{tn} \\ g_{nn} - G_{nn} \end{bmatrix}, \qquad \bar{\mathbf{S}} = \begin{bmatrix} S^{sn} \\ S^{tn} \\ S^{nn} \end{bmatrix} \tag{7}$$

3. Variational basis and finite element formulation

3.1. Weak form of equilibrium

The total potential energy Π_T of the system is given by the internal contribution due to the continuum adjacent bodies (bulks) $\Pi_{\text{int, bulk}}$, the internal contribution of the interface $\Pi_{\text{int, cohe}}$ and by the external applied actions Π_{ext}:

$$\Pi_T(\mathbf{u}) = \Pi_{\text{int, bulk}}(\mathbf{u}) + \Pi_{\text{int, cohe}}(\mathbf{u}) + \Pi_{\text{ext}}(\mathbf{u}) \tag{8}$$

The virtual variation of the energy balance equation takes the form:

$$\delta\Pi_T = \delta\Pi_{\text{int, bulk}}(\mathbf{u}) + \delta\Pi_{\text{int, cohe}}(\mathbf{u}) + \delta\Pi_{\text{ext}}(\mathbf{u}). \tag{9}$$

Excerpt from ISBN 978-3-00-053387-7

In what follows, we restrict the attention to the analysis of the internal contribution of the interface. In the reference configuration, the variation of the term corresponding to the internal interface energy is given by:

$$\delta\Pi_{\text{int, cohe}}(\mathbf{u}, \delta\mathbf{u}) = \int_{\bar{\mathcal{B}}_0} \bar{\mathbf{S}} : \delta\bar{\mathbf{E}} \, \mathrm{d}\Omega, \tag{10}$$

where $\delta\bar{\mathbf{E}}$ and $\bar{\mathbf{S}}$, Eq.(7), are the virtual strain vector and the stress vector whose relationship is governed by the constitutive law outlined in Section 4.

The virtual variation of the modified Green-Lagrange strain tensor concerning the interlaminar components yields

$$\delta\bar{\mathbf{E}} = \begin{bmatrix} \delta\bar{\mathbf{g}}_s \cdot \bar{\mathbf{g}}_n + \bar{\mathbf{g}}_s \cdot \delta\bar{\mathbf{g}}_n \\ \delta\bar{\mathbf{g}}_t \cdot \bar{\mathbf{g}}_n + \bar{\mathbf{g}}_t \cdot \delta\bar{\mathbf{g}}_n \\ \delta\bar{\mathbf{g}}_n \cdot \bar{\mathbf{g}}_n + \bar{\mathbf{g}}_n \cdot \delta\bar{\mathbf{g}}_n \end{bmatrix} \tag{11}$$

The variation of the metric components are computed through the variation of the displacements associated with the interface.

3.2. Finite element discretization

The standard finite element approach following an iso-parametric map introduces the discretization of the interface through $n_e \in \mathbb{N}$ solid shell-like interface elements. Using the typical tri-linear shape functions $N_A = N_A(\boldsymbol{\xi})$, which for the solid-shell kinematic description read [14]:

$$N_A = N_A(\boldsymbol{\xi}) = \frac{1}{8}\left(1 + \xi^1\xi^1_A\right)\left(1 + \xi^2\xi^2_A\right)\left(1 + \xi^3\xi^3_A\right) \quad \mathrm{A} = 1, \ldots, 8 \tag{12}$$

with $\boldsymbol{\xi}$ denoting the isoparametric domain. The position vectors of any material point in the reference and current configurations read:

$$\mathbf{X} \approx \sum_{A=1}^{n_n} N_A\mathbf{X}_A; \quad \mathbf{x} \approx \sum_{A=1}^{n_n} N_A\mathbf{x}_A \tag{13}$$

The real, virtual and incremental displacement vectors are interpolated via the shape functions as:

$$\mathbf{u} \approx \sum_{A=1}^{8} N_A\mathbf{d}_A = \mathbf{N}\mathbf{d}; \quad \delta\mathbf{u} \approx \sum_{A=1}^{8} N_A\delta\mathbf{d}_A = \mathbf{N}\delta\mathbf{d}; \quad \Delta\mathbf{u} \approx \sum_{A=1}^{8} N_A\Delta\mathbf{d}_A = \mathbf{N}\Delta\mathbf{d}, \tag{14}$$

where $\mathbf{N}$ and $\mathbf{d}$ are suitable operators that collect the interpolation functions and the nodal displacements of the element, whereas $\mathbf{d}_A$, $\delta\mathbf{d}_A$ and $\Delta\mathbf{d}_A$ stand for the nodal real, virtual and incremental displacement vectors. The virtual and incremental strain vectors are accordingly defined as:

$$\delta\bar{\mathbf{E}} = \sum_{A=1}^{8} \mathbf{B}_A\delta\mathbf{d}_A = \mathbf{B}\delta\mathbf{d}; \quad \Delta\bar{\mathbf{E}} = \sum_{A=1}^{8} \mathbf{B}_A\Delta\mathbf{d}_A = \mathbf{B}\Delta\mathbf{d}, \tag{15}$$

where $\mathbf{B}$ denotes the strain-displacement operator. The insertion of the expressions (13-15) into the weak form of the term associated with the internal energy of the interface (10) yields

$$\delta\Pi^h_{\text{int, cohe}}(\mathbf{d}, \delta\mathbf{d}) = \delta\mathbf{d}^{\mathrm{T}}\left[\int_{\bar{\mathcal{B}}_0} \mathbf{B}(\mathbf{d})^{\mathrm{T}}\bar{\mathbf{S}} \, \mathrm{d}\Omega\right] = \delta\mathbf{d}^{\mathrm{T}}\mathbf{R}, \tag{16}$$

where $\mathbf{R}$ is the residual vector at the element level.

Excerpt from ISBN 978-3-00-053387-7

The consistent linearization of (16) through the use of the directional derivative concept in the direction $\Delta\mathbf{d}$ is given by

$$\Delta\delta\Pi^{h}_{\text{int, cohe}}(\mathbf{d},\delta\mathbf{d},\Delta\mathbf{d}) = \delta\mathbf{d}^{\mathrm{T}}\left[\int_{\bar{\mathscr{B}}_0}\left(\frac{\partial\mathbf{B}(\mathbf{d})}{\partial\mathbf{d}}\right)^{\mathrm{T}}\bar{\mathbf{S}}\,\mathrm{d}\Omega + \int_{\bar{\mathscr{B}}_0}\mathbf{B}(\mathbf{d})^{\mathrm{T}}\Delta\bar{\mathbf{S}}\,\mathrm{d}\Omega\right]\Delta\mathbf{d} = \delta\mathbf{d}^{\mathrm{T}}\,[\mathbf{K}]\,\Delta\mathbf{d}, \tag{17}$$

where $\mathbf{K}$ denotes the element stiffness matrix.

The linearization of the stress vector can be accomplished using the material tangent modulus $\mathbb{C}_c$ of the interface (see Section 4) as follows

$$\int_{\bar{\mathscr{B}}_0}\mathbf{B}^{\mathrm{T}}(\mathbf{d})\Delta\bar{\mathbf{S}}\,\mathrm{d}\Omega = \int_{\bar{\mathscr{B}}_0}\mathbf{B}^{\mathrm{T}}(\mathbf{d})\mathbb{C}_c\mathbf{B}(\mathbf{d})\,\mathrm{d}\Omega, \quad \text{with } \mathbb{C}_c = \frac{\partial\bar{\mathbf{S}}}{\partial\bar{\mathbf{E}}} \tag{18}$$

Inserting (18) into the definition of the element stiffness matrix (17), one can identify the material $\mathbf{K}_{\text{mat}}$ and geometrical $\mathbf{K}_{\text{geom}}$ contributions to the stiffness matrix which are given by

$$\mathbf{K}_{\text{mat}} = \int_{\bar{\mathscr{B}}_0}\mathbf{B}^{\mathrm{T}}(\mathbf{d})\mathbb{C}_c\mathbf{B}(\mathbf{d})\,\mathrm{d}\Omega; \quad \mathbf{K}_{\text{geom}} = \int_{\bar{\mathscr{B}}_0}\left(\frac{\partial\mathbf{B}(\mathbf{d})}{\partial\mathbf{d}}\right)^{\mathrm{T}}\bar{\mathbf{S}}\,\mathrm{d}\Omega \tag{19}$$

Note that in case of geometrically linear applications, the reference and the current configurations are assumed to be coincident, leading to a vanishing geometrical contribution to the element stiffness matrix.

4. Interface law

4.1. Constitutive formulation

The simulation of delamination effects at the interface requires the incorporation of a suitable inelastic constitutive law. For a clear identification of the contribution of the intelaminar components of the Green–Lagrange strain tensor and of the second Piola-Kirchhoff stress tensor to the fracture modes I, and II, and III, the following notation is adopted:

$$\bar{\mathbf{E}} = \left[\bar{E}_{sn}, \bar{E}_{tn}, \bar{E}_{nn}\right]; \quad \bar{\mathbf{S}} = [S_{II}, S_{III}, S_I]^{\mathrm{T}} \tag{20}$$

In this contribution, the so-called Linear Elastic Brittle Interface Model (LEBIM) is employed [15]. This interface model attains a continuous distribution of linear springs, whose behavior at any material point can be defined as:

$$\begin{cases} S_I(x) = k_n E_I(x) \\ S_{II}(x) = k_s E_{II}(x) \\ S_{III}(x) = k_t E_{III}(x) \end{cases} \rightarrow \text{ for } \mathcal{G}(x) \le \mathcal{G}_c, \tag{21}$$

where S_I, S_{II}, S_{III} identify the normal and the tangential out-of-plane stress components, respectively; E_I, E_{II} and E_{III} are the normal and transverse shear strain components; the normal and shear stiffness of the spring distribution are denoted by k_n, k_s and k_t, respectively, and $\mathcal{G}(x) = \mathcal{G}_I(x) + \mathcal{G}_{II}(x) + \mathcal{G}_{III}(x)$. The Energy Release Rates (ERRs) at material point level that are associated with the fracture modes I ($\mathcal{G}_I(x)$), II ($\mathcal{G}_{II}(x)$) and III ($\mathcal{G}_{III}(x)$) can be computed as follows:

$$\mathcal{G}_I(x) = \frac{1}{2}\langle S_I\rangle E_I; \quad \mathcal{G}_{II}(x) = \frac{1}{2}S_{II}E_{II}; \quad \mathcal{G}_{III}(x) = \frac{1}{2}S_{III}E_{III}, \tag{22}$$

where $\langle\bullet\rangle$ denotes the Macauley bracket of the magnitude $\bullet$ to account for only tensile mode I for decohesion. Under mixed mode, the interface failure is assessed using the 3D version of the Benzeggah-Kenane failure criterion [16], that reads

$$G_c = G_{Ic} + (G_{IIc} - G_{Ic})\left(\frac{G_{II} + G_{III}}{G_I + G_{II} + G_{III}}\right)^{\eta} \tag{23}$$

Excerpt from ISBN 978-3-00-053387-7

where η is a fitting parameter with respect to the single mode experiments, namely double cantilever beam (DCB) and end notch flexure (ENF) for mode I and mode II conditions, respectively, and mixed mode bending (MMB) for mixed mode scenarios. However, note that any different fracture criterion can be implemented into the present formulation in a straightforward manner.

Figure 2 depicts the linear single response corresponding to the modes I and II of the LEBIM, where S_I^0 and S_{II}^0 denote the fracture strength for modes I and II, respectively and E_I^0 and E_{II}^0 denote the corresponding strains. The area under the effective stress-strain curve is set equal to the fracture toughness of each mode divided by the initial interface thickness H_0. Thus, for one arbitrary fracture mode m ($m = I, II, III$), the corresponding fracture toughness can be computed as: $\mathcal{G}_{mc}^* = \mathcal{G}_{mc}(x)/H_0$. Taking the linear stress-strain relation, the fracture toughness corresponding to each individual fracture mode reads:

$$\mathcal{G}_{Ic}^* = \frac{(\langle S_I \rangle)^2}{2k_n}; \quad \mathcal{G}_{IIc}^* = \frac{(S_{II})^2}{2k_{II}}; \quad \mathcal{G}_{IIIc}^* = \frac{(S_{III})^2}{2k_{III}} \tag{24}$$

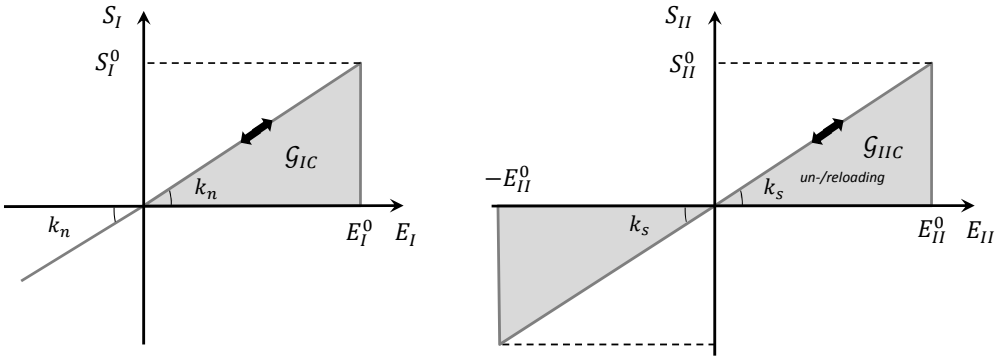

Figure 2. Interface response corresponding to the fracture mode I (left) and II (right) according to the LEBIM.

4.2. Benchmark example

The proposed interface element formulation is assessed by means of a single interface element between 2 isotropic bulk elements ($E = 210$GPa, $\nu = 0.3$) subjected to simple tensile loading (mode I). The mechanical properties of the interface are reported in Table 1. Figure 3 shows the reaction force–displacement evolution curve corresponding to this numerical tests, whereby a clear nonlinear reaction-displacement curve is obtained before the abrupt failure. However, in case the geometrical nonlinear effects are removed from the interface formulation, a fully linear elastic interface response is recovered.

Table 1. Fracture properties of the benchmark mode I test

G_{Ic} [J/mm^2]	$G_{IIc} = G_{IIIC}$ [J/mm^2]	k_n [GPa]	k_s [GPa]	k_t [GPa]	η
270	270	450	450	450	2

5. Concluding remarks

In this contribution, a nonlinear finite thickness interface model has been proposed. The current element formulation relied on the degeneration of the solid shell concept. With regard to the interface behavior,

Excerpt from ISBN 978-3-00-053387-7

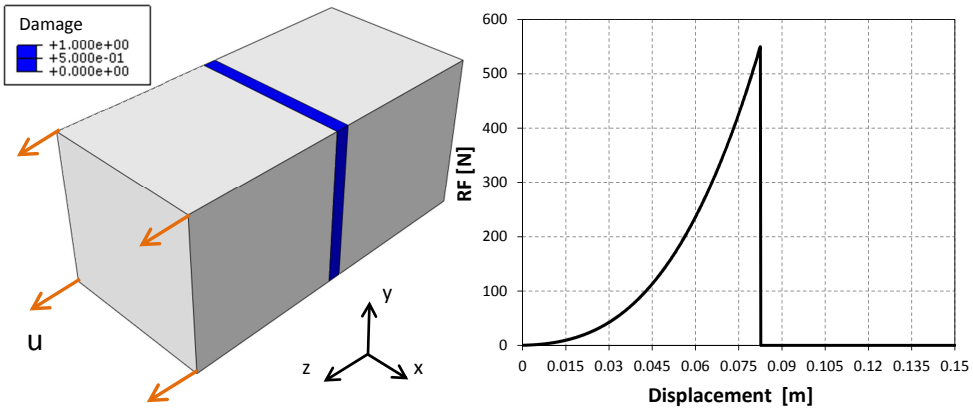

Figure 3. Nonlinear LEBIM response for pure mode I loading conditions, see Table 1 for mechanical properties.

an extension of the LEBIM model has been incorporated into the current model. A simple benchmark problem has been used in order to assess the element response under pure mode I fracture. This application showed that the geometric effects into the interface element formulation led to a nonlinear response prior to abrupt failure. The capabilities of the current model will be further investigated through more complex applications concerning engineering structures.

Acknowledgments

JR and AB acknowledges the Spanish Ministry of Economy and Competitiveness/FEDER (DPI2012-37187) and the Andalusian Government (Projects of Excellence No. TEP-7093 and P12-TEP-1050). MP acknowledges the European Research Council for the support to the ERC Starting Grant "Multi-field and multi-scale Computational Approach to Design and Durability of PhotoVoltaic Modules" - CA2PVM, under the European Union's Seventh Framework Programme (FP/2007-2013)/ERC Grant Agreement n. 306622.

References

[1] Krueger R (2002) The virtual crack closure technique: history, approach and applications. NASA/CR-2002-211628.

[2] Dugdale D (1960) Yielding of steel sheets containing slits. J Mech Phys Solids 8(2):100–104.

[3] Barenblatt G (1962) The mathematical theory of equilibrium cracks in brittle fracture. Adv. Appl. Mech. 7, 55-129, 1962.

[4] Camanho PP, Dávila CG, de Moura MF (2003). Numerical simulation of mixed-mode progressive delamination in composite materials. J. Compos. Mater. 37, 1415–1438.

[5] Harper PW, Hallett SR (2008) Cohesive zone length in numerical simulations of composite delamination. Eng Fract Mech, 75(16):4774–4792.

[6] Allix O, Corigliano A, 1999. Geometrical and interfacial non-linearities in the analysis of delamination in composites. Int J Solids Struct 36, 2189–2216.

Excerpt from ISBN 978-3-00-053387-7

[7] Ortiz M, Pandolfi A (1999) Finite-deformation irreversible cohesive elements for three-dimensional crack-propagation analysis. Int J Num Meth Eng 44:1267–1282.

[8] de Borst R, Schipperen JHA (2002)Computational methods for delamination and fracture in composites. In: Allix O, Hild F, editors. Continuum damage mechanics of materials and structures. Elsevier Science Ltd. p. 325–352.

[9] van den Bosch MJ, Schreurs PJG, Geers MGD (2007) A cohesive zone model with a large displacement formulation accounting for interfacial fibrilation. European J Mech A/Solids 26:1–19.

[10] Reinoso J, Paggi M (2014) A consistent interface element formulation for geometrical and material nonlinearities, Comput Mech, 54:1569–1581.

[11] Balzani C, Wagner W (2008) An interface element for the simulation of delamination in unidirectional fiber-reinforced composite laminates. Eng Fract Mech 75:2597–615.

[12] Paggi M, Wriggers P (2012) Stiffness and strength of hierarchical polycrystalline materials with imperfect interfaces. J Mech Phys Solids 60:557–572.

[13] Corrado M, Paggi M (2014) Nonlinear fracture dynamics of laminates with finite thickness adhesives. Mech Mater 80B:183–192.

[14] Reinoso J, Paggi M, Areias P (2016) A finite element framework for the interplay between delamination and buckling of rubber-like bi-material systems and stretchable electronics. J Eur Ceram Soc (2016), http://dx.doi.org/10.1016/j.jeurceramsoc.2016.01.002.

[15] Reinoso J, Blázquez A, Távara L, París F, Arellano C (2016) Damage tolerance of composite runout panels under tensile loading. Comp Part B: Engineering, accepted for publicaion.

[16] Benzeggagh ML, Kenane M. (1996) Measurement of mixed-mode delamination fracture toughness of unidirectional glass/epoxy composites with mixedmode bending apparatus. Comp Sci Tech 56(4):43949.

Excerpt from ISBN 978-3-00-053387-7